Frontiers in Bioscience Landmark

Front. Biosci. (Landmark Ed) **2025**; 30(7): 39679
https://doi.org/10.31083/FBL39679

Original Research

Comprehensive Identification and Unveiling Key Nitrate-Transporting Proteins in Oat (*Avena sativa* L.)

Rong Cheng[1,2,†], Qiang Xiao[3,†], Jie Gong[2], Renwei Sun[4], Yinke Du[1,2], Wei Zhao[2], Wei Zheng[1,*], Shiqing Gao[2,*]

[1]College of Grassland Science, Xinjiang Agricultural University, 830052 Urumqi, Xinjiang, China
[2]Institute of Hybrid Wheat, Beijing Academy of Agriculture and Forestry Sciences, 100097 Beijing, China
[3]Institute of Plant Nutrition, Resources and Environment, Beijing Academy of Agriculture and Forestry Sciences, 100097 Beijing, China
[4]Laboratory of Plant Breeding and Genetics, Department of Agricultural and Environmental Biology, The University of Tokyo, 113-8657 Tokyo, Japan
*Correspondence: zw065@163.com (Wei Zheng); gshiq@126.com (Shiqing Gao)
[†]These authors contributed equally.
Academic Editor: Jen-Tsung Chen
Submitted: 11 April 2025 Revised: 22 June 2025 Accepted: 30 June 2025 Published: 29 July 2025

Abstract

Background: Nitrate transporter NRT1/PTR family (NPF) proteins are crucial for plant nitrogen uptake and utilization. As an important hexaploid crop for grain and forage, oat (*Avena sativa* L.) requires substantial levels of nitrogen. However, the oat nitrate transporter 1 (NRT1) family remains uncharacterized. **Methods**: In this study, the oat *NRT1* subfamily members were identified through the Hmm and Pfam databases. Bioinformatics analysis was performed using the MEGA 11 and TBtools software to elucidate the physicochemical properties, evolutionary relationships, chromosomal localization, and gene structures. Furthermore, quantitative real-time polymerase chain reaction (qRT-PCR) analysis and the green fluorescent protein (GFP) fusion expression vector were utilized to investigate the candidate oat *NRT1s*. **Results**: Phylogenetic classification categorized oat *NRT1s* into eight subfamilies, with the most abundant being the NPF5 subfamily. Physicochemical property analysis revealed that the number of amino acids in the proteins encoded by these genes ranged from 235 to 673, with their molecular weights (MWs) ranging from 26 kDa to 74 kDa. Chromosomal localization revealed that these genes were unevenly distributed across all 12 oat chromosomes. Promoter analysis revealed that light-responsive elements appeared most frequently in the promoters of these genes (39.3%), followed by abscisic acid (ABA)-responsive elements (13.5%) and methyl jasmonate (MeJA)-responsive elements (9.4%). qRT-PCR analysis revealed that most of the genes exhibited tissue-specific expression patterns. Among them, *AsNPF2.6* was highly expressed in the leaves at 1 h post-low nitrogen (LN) treatment, while *AsNPF4.5* was highly expressed in the leaves at 12 h. Both these genes exhibited low expression levels in the roots. However, *AsNPF7.16* and *AsNPF7.19* were both highly expressed in the roots at 9 h post-LN treatment but exhibited low expression in the leaves. Subcellular localization revealed that all five proteins (AsNPF2.6, AsNPF4.5, AsNPF7.16, AsNPF6.8, and AsNPF7.19) were localized to the cytoplasm and cell membrane. **Conclusions**: Our results demostrate the involvement of *AsNRT1* family members in nitrogen transport in oat, providing theoretical support for further investigation into the functions and molecular mechanisms of action of oat *NRT1s* in nitrogen transport.

Keywords: *Avena*; nitrate transporters; nitrogen; phylogeny; genomics; cluster analysis

1. Introduction

Nitrogen is the most demanded nutrient element by plants and is a key limiting factor for plant growth [1,2]. However, currently, only developed countries have a nitrogen fertilizer utilization rate of 50–60% [3], while developing countries, such as India [4] and Brazil [5], have an average nitrogen fertilizer utilization rate of only 30–40%. The low utilization rate of nitrogen fertilizer not only leads to a waste of resources and economic losses but also causes a series of environmental problems, including acidification of soil crusts, eutrophication of water bodies, nitrate contamination of groundwater, and intensification of greenhouse gas emissions [6,7]. Therefore, fully exploring the potential of plants to enhance their nitrogen utilization efficiency is a key issue that must be addressed in contemporary agricultural production.

The primary form of nitrogen that plants obtain from the soil is nitrate, and nitrate transport proteins primarily facilitate the uptake and transportation of this essential nutrient [8,9]. Nitrate is a key component of plant-synthesized proteins, chlorophyll, and various other compounds. Additionally, nitrate stored in vesicles plays an important role in ion homeostasis and osmoregulation. The nitrate transporter 1 family (NRT1/PTR family, abbreviated as NPF family) is the largest nitrate transporter protein group in plants, mainly responsible for the transport of nitrate and plant hormones [10,11].

In the dicotyledonous plant *Arabidopsis thaliana*, the NPF family comprises 53 *NRT1* members [12]. Among these, 11 proteins have been reported as essential for nitrogen uptake and transport in *Arabidopsis thaliana* [13,14]. For instance, *AtNRT1.1* (*AtNPF6.3*) represents a seminal

discovery within the NRT1 protein family, playing a crucial role in nitrate uptake by plants [15]. *AtNRT1.1* (*AtNPF6.3*) is an integral part of the signaling cascade response and is actively involved in coordinating the adaptive response of plants to fluctuating nitrate concentrations in the environment, highlighting its significance for sustainable plant growth and nutrition [16]. Furthermore, *AtNRT1.4* is involved in regulating nitrate homeostasis in the leaves and affecting the leaf development processes [17], while *AtNRT1.5* is responsible for mediating nitrate transport from roots to aboveground parts [18]. In addition, *AtNRT1.6* is involved in regulating early embryonic development processes in plants [19]. *AtNRT1.7* promotes the transport of nitrate between old and young leaves and participates in its reuse process, while *AtNRT1.9* is responsible for the transport of nitrate to the base through the phloem [20]. Notably, the expression levels of these genes are induced by nitrate ions (NO_3^-) and are strongly regulated by phytohormones. However, few studies have examined the relationship between *NRT1* and NO_3^- in crops other than wheat and rice, primarily due to the research limitations associated with non-model plants in terms of mutant materials and gene-cloning technology. Previously, response characteristics of *NRT1.1* and *NRT1.2* under different nitrogen supply conditions have been investigated in wheat [21], and the biological function of *OsNRT1.1* has been elucidated in rice [22].

Low nitrogen utilization efficiency is a significant constraint on the sustainable development of oat (*Avena sativa* L.). Screening and characterizing key nitrate transporter genes is crucial for breeding nitrogen-efficient oat varieties. While oat quality is largely determined by its genetics, it is also influenced by the external environment. Oat is often grown in arid and infertile soils and is commonly fertilized with NH_4^+. This practice can lead to stunting during the early reproductive stages of the plant due to the slow biotransformation of NH_4^+ caused by low soil temperatures in early spring. Incorporating a certain percentage of NO_3^- into the nitrogen fertilizer might promote early oat development [23,24]. Nitrogen fertilizers are critical in dry matter accumulation, morphology establishment, and fresh grass yield quality of oat [25,26]. At present, there is an imbalance between forage supply and demand, and with the continuous development of animal husbandry, the demand for forage is increasing. Excessive application of nitrogen fertilizers to increase forage production results in the production of large amounts of ammonium nitrogen, which wastes resources and increases the pressure on the environment. Therefore, it is imperative to explore the cloning of nitrogen transporter genes for various molecular improvements and yield increases.

The whole genome sequencing of oat has been successfully completed [27]; however, the function of the *NRT1* family in oat growth and development is still unclear. At present, there are few research reports on the response patterns of the members of this family under different nitrogen treatment conditions and their mechanisms of action in maintaining nitrogen homeostasis in oat. Therefore, in the present study, we identified the oat *NRT1* family members and performed bioinformatics analysis and gene cloning of several candidate genes involved in nitrate uptake and transport. Our findings provide excellent genetic resources for oat nitrogen-efficient molecular breeding and are important for the high and stable yield of oat.

2. Materials and Methods

2.1 Identification and Physicochemical Characterization of NRT1 Genes (NRT1s) in Oat

The sequences of oat proteins were downloaded from the Ensembl Plants database (https://plants.ensembl.org/index.html) [28] and was used to build a local protein database. Subsequently, a hidden Markov model (PF00854) of the *NRT1* family was obtained from the Pfam database, and the local database was searched using the HMMER v3.0 (Sean Eddy, Seattle, WA, USA) (E value $< 10^{-10}$) to preliminarily screen oat NRT1 proteins (NRT1s) and remove redundant sequences [29,30]. The screened sequences were submitted to the NCBI protein Batch CD-search database (https://www.ncbi.nlm.nih.gov/Structure/bwrpsb/bwrpsb.cgi) for conserved domain identification, and the sequences lacking conserved domains were removed accordingly [31]. The obtained oat *NRT1* family genes were renamed, specifically for each member, as NPFX.Y, where X denotes the subfamily, and Y denotes the member within the species. There were eight subfamilies of the genes.

Using the sequences of 53 *NRT1s* involved in nitrate uptake and transport in *Arabidopsis thaliana*, *Oryza sativa* L., *Zea mays* L., and *Setaria italica* miltiorrhiza as probes, homologous sequence searches were conducted with the oat whole genome database using BLASTP (https://blast.ncbi.nlm.nih.gov/Blast.cgi). Combined with phylogenetic tree analysis, 197 oat *NRT1s* were ultimately identified. Chromosomal localization (including the start and end sites of the 197 oat *NRT1s* on the chromosome), encoded protein length, and other basic information of oat were obtained from the Ensembl Plants database (https://plants.ensembl.org/). The ExPASy platform (https://www.expasy.org/) was used to predict and analyze the molecular weight (MW), isoelectric point (pI), mean hydrophobicity value (grand average of hydropathicity value, abbreviated as GRAVY value), instability index, and lipid index of oat NRT1s [32]. The sequences of the proteins were submitted to the WoLF PSORT website (https://wolfpsort.hgc.jp/) [33] and Cell-PLoc 2.0 website (http://www.csbio.sjtu.edu.cn/bioinf/plant-multi/) [34] to predict their subcellular localization.

2.2 Construction of a Phylogenetic Tree for the Oat NRT1 Family

To elucidate the relationships of *NRT1*s between wheat and other species, a total of 197, 53, 3, 3, 3, and 8

NRT1 family members of oat, *Arabidopsis thaliana*, rice, maize, wheat, and *S. italica*, respectively, were obtained from the Ensembl Plants database and imported into MEGA 11 (MEGA Software, Tempe, AZ, USA) [35]. Phylogenetic analysis of *NRT1* family members was performed using the Clustal W multiple sequence alignment method combined with the neighbor-joining (NJ) method. When building a phylogenetic tree, the bootstrap value was set to 1000, and the default configuration was used for all other parameters. The Newick (NWK) format file of the phylogenetic tree generated by the MEGA 11 software has been uploaded to the Evolview online platform (https://evolgenius.info//evolview-v2/#login) to optimize the visualization effect [36].

2.3 Chromosomal Location and Covariance Analysis of Oat NRT1 Family Members

Using the "GTF/GFF Gene Localization Visualization" plugin in TBtools (CJ Chen, Guangzhou, Guangdong, China), the physical location information of oat *NRT1* family members was input [37], and the gene localization map on chromosomes was generated and exported. The covariance relationships among oat, *Arabidopsis thaliana*, and rice genomes were analyzed using the MCscanX plugin in the TBtools software. A total of 197 *AsNRT1s* were highlighted, and covariance maps among genomes were plotted.

2.4 Structural Characteristics and Conserved Motif Analysis of NRT1 Family Members in Oats

Exon-intron structure information was obtained from the oat genome annotation file using the "Visualize Gene Structure" tool from TBtools [37]. The AsNRT1 protein sequence was submitted to the MEME online tool (https://meme-suite.org/meme/tools/meme) to perform conservative motif prediction with the following parameter settings: The number of motifs was set to 15, and the length of motifs was set within the range of 6–100 amino acid residues. Subsequently, TBtools was used to visualize and analyze the predicted gene structure and conserved motifs [37,38].

2.5 Analysis of Cis-Acting Elements in Oat NRT1 Family Members

The regulatory sequence 2000 bp upstream of the transcription start site of *AsNRT1* was extracted using the "GXF Sequence Extraction" tool in TBtools and submitted to the PlantCARE database (http://bioinformatics.psb.ugent.be/webtools/plantcare/html/) to analyze the cis-acting components [39]. The cis-acting elements in the *AsNRT1s* were analyzed, and the results were categorized according to the function of the elements and visualized using TBtools.

2.6 Analysis of the Expression Patterns of Oat NRT1 Family Members in Different Tissues

The coding sequences (CDSs) of all *AsNRT1s* in oat were extracted and compared with the diploid oat (*A. longiglumis*) CDS database, retaining the diploid oat genes with the highest matching degree to the oat *AsNRT1s*. Based on the diploid oat expression database (http://db.ncgr.ac.cn/oat/newel.php) by matching the gene names, the expression levels of *NRT1s* in different tissues of diploid oat (including root tips, roots, leaves, stems, spikes, and spikelets) were obtained (represented by the number of fragments per kilobase transcript read per million mapped reads, abbreviated as FPKM value), and a gene expression clustering heat map was drawn using the TBtools software.

2.7 Plant Materials and Growth Conditions

The seeds of Bailyan VII oat material used in this experiment were provided by Prof. Zhao Guiqin of Gansu Agricultural University. It is suitable for cultivation in arid and semi-arid areas, alpine shady and humid areas, second-shade areas and similar ecological zones in central Gansu. After soaking the seeds in a 1% hydrogen peroxide solution for 3 min for surface disinfection, they were rinsed thrice with deionized water and then soaked in deionized water for 12 h. Post-soaking, the seeds were evenly arranged in petri dishes lined with moistened filter paper, oriented with ventral grooves facing downward. Seed germination was induced in the dark at 22 °C, with periodic moisture application by spraying deionized water. The germinated seeds were transferred to a light-controlled incubator supplemented with Hoagland nutrient solution for cultivation. The cultivation conditions were set as follows: relative humidity of 65%, light/dark period of 16 h/8 h, light period temperature of 22 °C, dark period temperature of 16 °C, and light intensity of 200–250 $\mu mol \cdot m^{-2} \cdot s^{-1}$. Forty plants were established, with 20 seedlings per treatment group. The nutrient solution was replaced every 72 h. When the seedlings reached the two-leaf and one-heart development stage, they were divided into two groups: The control (CK) group, treated with 20 mM nitrogen, and the low nitrogen (LN) group, treated with 2 mM nitrogen. The leaf and root tissue samples were collected at 0, 1, 3, 6, 9, 12, and 24 h post-processing. Immediately after sample collection, three plants per time point were placed in liquid nitrogen for quick freezing and then transferred to a –80 °C freezer for long-term storage.

2.8 RNA Extraction and Quantitative Real-Time Polymerase Chain Reaction (qRT-PCR) Analysis

Total RNA was extracted from plant tissues using the RNAprep Pure Plant Total RNA Extraction Kit (B0226B, Tiangen Biochemical Technology, Beijing, China) for subsequent analysis of target gene expression. The Eco Real Time PCR system (Illumina, San Diego, CA, USA) was used for quantitative real-time polymerase chain reaction (qRT-PCR), with oat actin gene (*AsActin*) as the internal reference gene [40]. The primers used for qRT-PCR are shown in **Supplementary Table 1**.

2.9 Subcellular Localization in Wheat Protoplasts

Gene-specific primers were used to amplify the *NRT1* CDS and clone it into the N-terminus of green fluorescent protein (GFP) in GFP expression vector (16318h-GFP-NOS). Protoplasts were isolated from wheat seedling leaves as described previously [41]. The recombinant plasmid 16318h-NRT1-GFP and the empty vector control 16318h-GFP were introduced into wheat protoplasts using the polyethylene glycol (PEG)-mediated transformation method [41]. The transfected protoplasts were cultured in the W5 solution at 23 °C for 18 h in the dark. Then, the GFP fluorescence signal was observed using a laser scanning confocal microscope (8100001684, Leica Microsystems GmbH, Wetzlar, Germany). The primer sequences are listed in **Supplementary Table 2**.

2.10 Statistical Analysis

qRT-PCR data were normalized using actin, with vertical bars representing standard deviation. Significant differences in the variables were indicated by $p < 0.05$, $p < 0.01$, $p < 0.001$, and $p < 0.0001$. All data processing and statistical analysis were performed using GraphPad Prism 7.0 (GraphPad Software Inc., San Diego, CA, USA).

3. Results

3.1 Identification and Physicochemical Characterization of the NRT1 Family in Oat

Through HMMER whole genome scanning combined with Conserved Domains Database (CDD) (https://www.ncbi.nlm.nih.gov/Structure/cdd/wrpsb.cgi) conserved domain validation, a total of 197 oat *NRT1* family members with complete PF00854 (PTR2) domain were identified. Subsequent screening via BLASTP alignment validated these 197 oat *NRT1s*. These genes encoded proteins ranging in size from 235 amino acids (AsNPF8.40) to 673 amino acids (AsNPF2.2) with MWs varying between 26 kDa (AsNPF8.40) and 74 kDa (AsNPF2.2) (**Supplementary Table 3**). Bioinformatic analysis revealed that the pIs of the proteins ranged from 4.89 (AsNPF8.28) to 11.06 (AsNPF7.4), indicating a broad range of acidic to basic properties within the NPF family.

Among the 197 identified *NRT1s*, 131 exhibited instability indices below 40, classifying them as stable proteins (**Supplementary Table 3**). Hydrophobic analysis showed that the average GRAVY value of the 195 proteins was positive, indicating that these proteins had hydrophobicity. Notably, only two proteins, AsNPF4.21 and AsNPF5.10, showed negative GRAVY values, indicating hydrophilic properties. Subcellular localization analysis using the Cell-PLoc 2.0 and the WoLF PSORT web tool predicted that nearly all *AsNRT1s* localize to vesicle membranes. In addition, 25 proteins were localized to the cell membrane, 7 to the endoplasmic reticulum, and 1 to the mitochondria. Thus, we hypothesized that the *NRT1s* in oat might play varying roles in nutrient transport.

3.2 Phylogenetic Analysis of Oat NRT1 Family

A phylogenetic tree was constructed using the proteins from oat (*A. sativa*), rice (*O. sativa*), corn (*Z. mays*), common wheat (*Tritium aestivum* L.), *S. italica* and *A. thaliana* to analyze the evolutionary relationship of the oat *NRT1* family (Fig. 1). Based on the subfamily classification system of *Arabidopsis thaliana NRT1* family, phylogenetic analysis showed that the *NPF5* subfamily of oat was the most abundant subfamily (with 56 members) in the oat *NRT1* family, followed by the *NPF8* subfamily (with 47 members). The *NPF3* and *NPF1* subfamilies were the least abundant, with only 11 and 1 family member, respectively. Phylogenetic analysis also showed that oat *NRT1s* in the same subfamily had closer genetic relationships but farther genetic relationships with the members in other subfamilies. This finding suggested that the oat *NRT1* family might have undergone adaptive differentiation during its evolutionary process.

Next, we identified the genes in nitrate uptake and transport, including 11, 3, 3, and 8 genes in *S. italica* [42], *Arabidopsis thaliana* [15,19,43], *O. sativa* [44], and *Z. mays* [45], respectively. Phylogenetic analysis revealed distinct evolutionary relationships among oat NPFs. AsNPF2.1, AsNPF2.2, AsNPF2.4, AsNPF2.6, AsNPF2.7, AsNPF2.20, and AsNPF2.22 clustered closely with AtNPF2.11, exhibiting 89–95% sequence identity. AsNPF4.5, AsNPF4.18, and AsNPF4.23 were highly homologous to SiNPF4.6 (99%, 94%, and 99% identity, respectively). The AsNPF6.1–AsNPF6.3 subgroups demonstrated near-complete sequence conservation with OsNPF6.5 (99%, 92%, and 99% identity, respectively). AsNPF6.8, AsNPF6.13, and AsNPF6.14 clustered with SiNPF6.7 (93–97% identity). AsNPF6.9, AsNPF6.15, AsNPF6.16, and AsNPF6.17 aligned closely with OsNPF6.3 (93–95% identity). These proteins from the non-oat species were evolutionarily similar, with a high structural and functional similarity, and can be used as a reference for inferring the functions of oat NPF proteins.

3.3 Chromosomal Localization Analysis of Oat NRT1s

Chromosomal localization analysis showed that 197 *AsNRT1s* were unevenly distributed across the oat chromosomes (**Supplementary Fig. 1**). Among them, 58, 38, 28, 27, 22, 14, and 9 genes were located on chromosomes 4, 1, 2, 7, 6, 3, and 5, respectively. We also detected one unassigned scaffold Un25. Notably, chromosome 4 exhibited the highest *AsNRT1* density, with 23 *AsNRT1s* specifically clustered on its 4A subgenome.

3.4 Collinearity Analysis of Oat NRT1s

Through collinearity analysis of the 197 oat *NRT1s*, their chromosomal distribution patterns were analyzed, homologous gene pairs were identified, and evolutionary relationships were inferred to identify potential gene duplication events. To investigate the evolutionary mechanisms

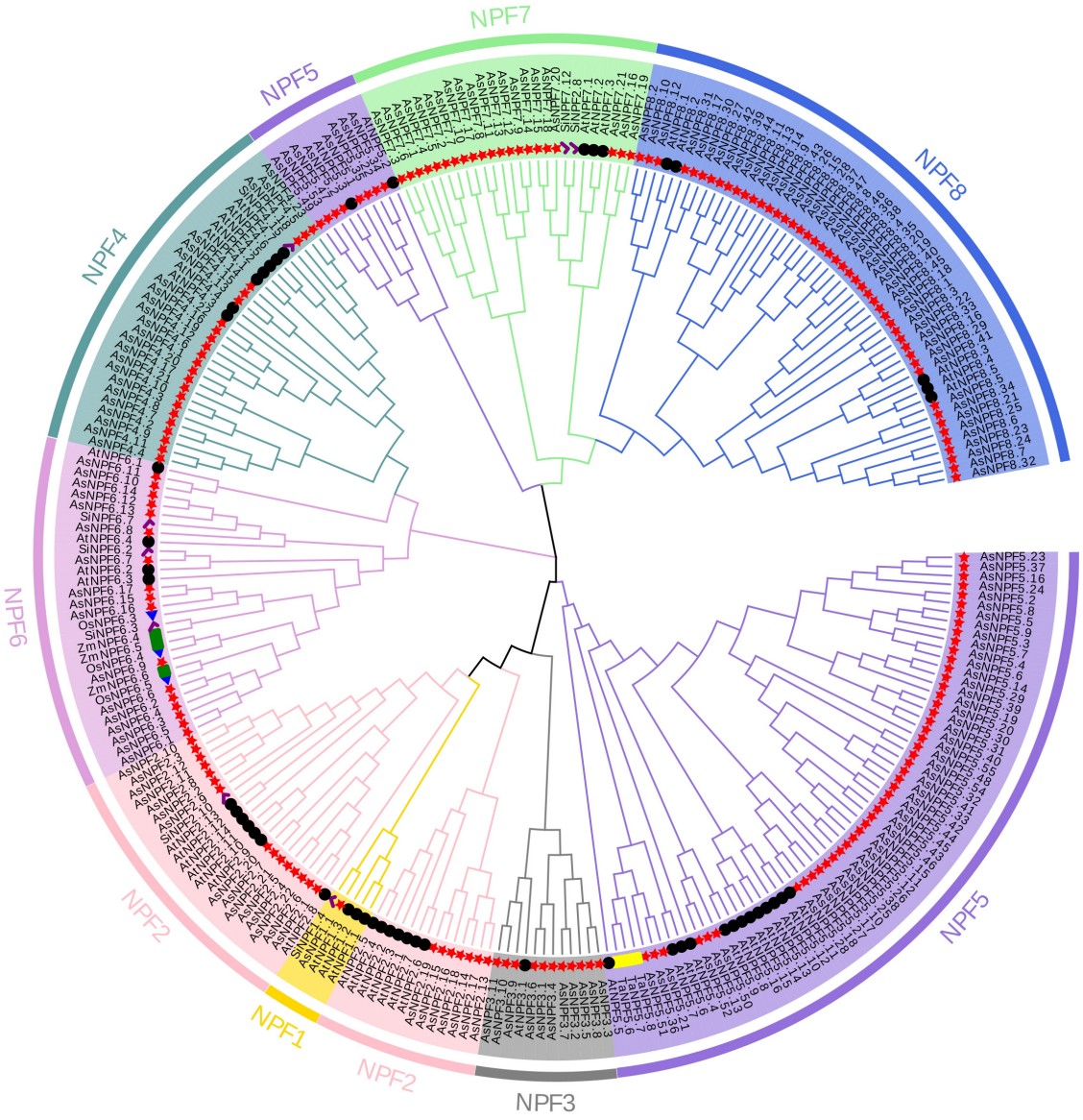

Fig. 1. Phylogenetic tree of NRT1s in monocots (*Avena sativa* L., *Triticum aestivum* L., *Oryza sativa* L., *Zea mays* L., and *Setaria italica.*) and a dicot (*Arabidopsis thaliana*). Oat NPF subfamilies are indicated by different colours: NPF1 (gold), NPF2 (pink), NPF3 (grey), NPF4 (cadet blue), NPF5 (medium purple), NPF6 (plum), NPF7 (light green), and NPF8 (royal blue). The red star, black circle, green rectangle, yellow strip, blue triangle, and purple check marks represent the AsNPFs, AtNPFs, ZmNPFs, TaNPFs, OsNPFs, and SiNPFs, respectively. NPF, nitrate transporter 1 family.

of the oat *NRT1* family, we generated a comparative phylogram within the genome of oat itself (Fig. 2a). To elucidate their evolutionary relationships with other species, we performed collinearity analysis of the 197 *AsNRT1s* across three species: The monocot *O. sativa*, diploid oat *A. longiglumis*, and the dicot *A. thaliana* (Fig. 2b). Our analysis revealed 114, 89, and 4 syntenic gene pairs with diploid oat, rice, and *Arabidopsis thaliana*, respectively. The differential number of conserved syntenic blocks reflects evolutionary divergence, with hexaploid oat *A. sativa* showing closer phylogenetic affinity to monocot rice than to the distantly related dicot *Arabidopsis thaliana*.

A 200-kb chromosomal region containing ≥2 genes is defined as a tandem duplication event [46]. Genomic analysis showed that 36 *AsNRT1s* clustered in 16 tandem repeat regions of oat linkage groups 1A, 1C, 1D, 2A, 2C, 2D, 3C, 4A, 4C, 4D, 5A, and 6A. Further analysis using BLASTP combined with MCScanX led to the identification of 81 fragment duplication events, involving 108 *AsNRT1s* (**Supplementary Table 4**). These results indicated that tandem and segmental repeats promoted the expansion of the *AsNRT1* family, with segmental repeats being the main driving force for the evolutionary diversity of this family.

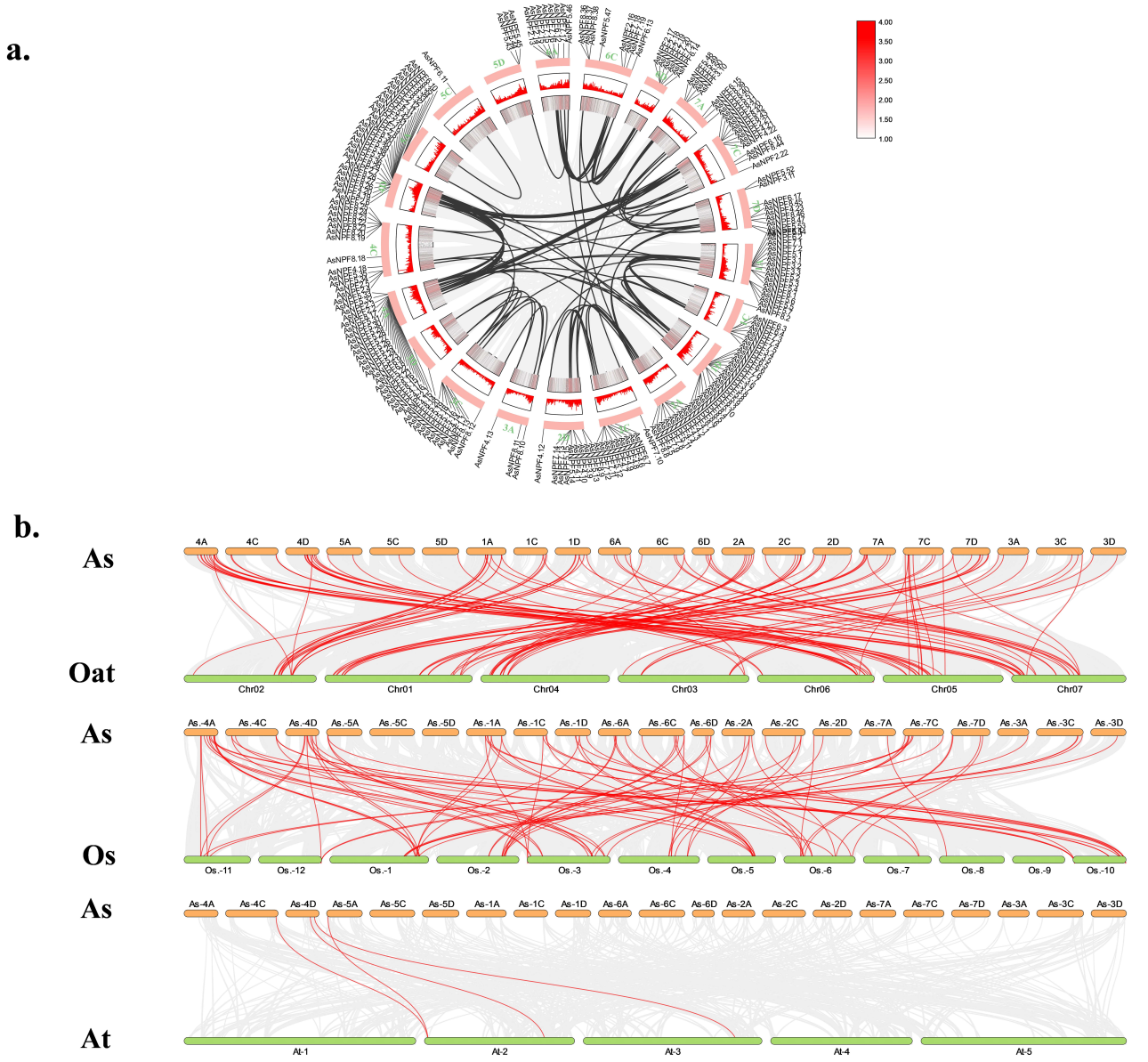

Fig. 2. Inter-species collinearity analysis of *NRT1s* in *Avena sativa* L., *Oryza sativa*, *Arabidopsis thaliana*, and *A. longigluis*. (a) Covariance analysis of *AsNRT1s* in the oat genome. The grey and black lines indicate all duplicated gene pairs in the oat genome and duplicate gene pairs among the 197 *AsNRT1s*, respectively. (b) Analysis of covariance between species of the *AsNRT1s*. The grey and red lines represent the region of co-collinearity between oat and other plants and the co-collinearity of *AsNRT1s*, respectively.

To analyze the evolutionary selection pressure on the *NRT1* family, we calculated the non-synonymous substitution rate (Ka), synonymous substitution rate (Ks), and Ka/Ks ratio of gene pairs (**Supplementary Table 5**). Among them, Ka/Ks of 1 indicated that the gene is in a neutral selection state, while Ka/Ks of <1 and >1 indicated negative and positive purification selections, respectively. Analysis of *AsNRT1* pairs with all fragment and tandem repeats showed that the Ka/Ks values of most orthologous gene pairs were <1, indicating that the oat *NRT1* family might have undergone a strong purification selection pressure during its evolution.

3.5 Structural Characteristics and Conserved Motifs of the Oat NRT1 Family

A phylogenetic tree based on the maximum likelihood (ML) method was constructed to analyze the structural domain characteristics of oat *AsNRT1s*. Firstly, ClustalW multiple sequence alignment was performed on the sequences of the 197 *AsNRT1s*, followed by phylogenetic analysis. The amino acid sequences of the *AsNRT1s* were submitted to the MEME database (Fig. 3). The evolutionary relationships among AsNRT1s were investigated based on their protein sequences, and the clustering results from the branches were consistent with those of *Arabidopsis thaliana*

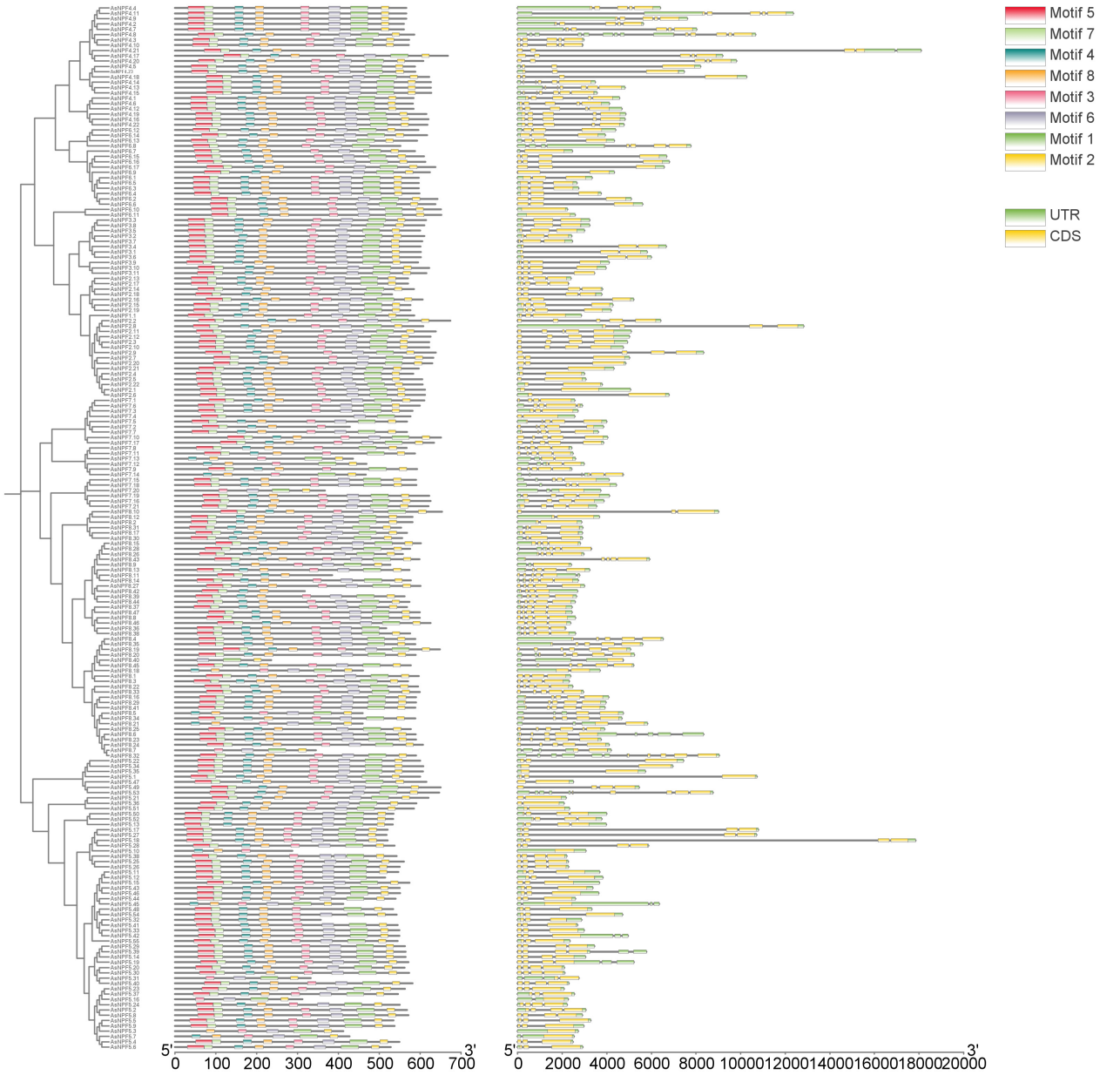

Fig. 3. Phylogenetic relationship and evolutionary trajectory analysis of *AsNRT1s*. Conservative motif analysis, annotated with different small boxes (each box representing an independent motif). In the genetic structure, introns are represented by black lines, while exons are distinguished by green and yellow boxes.

NRT1s. Using bioinformatic methods, a total of eight conserved motifs were identified in *AsNRT1s* and named motifs 1 to 8 (**Supplementary Fig. 2**).

To further investigate the evolutionary characteristics of the oat *NRT1* family, exon-intron structure analysis was performed on all identified *AsNRT1s* (Fig. 3). Our results showed that the number of exons in the genes of this family ranged from 1 to 6, with 10, 17, 55, 63, 52, and 3 genes containing 1, 2, 3, 4, 5, and 6 exons, respectively. By combining evolutionary trees and gene structures, we observed that the genes within the same group usually had similar structures.

3.6 Bioinformatic Analysis of the Cis-Acting Elements in the Promoter Regions of AsNRT1s

The promoter sequences of the 197 *AsNRT1s* were submitted to the PlantCARE database to identify cis-acting elements to elucidate the transcriptional regulatory mechanisms of this gene family. As a key binding region of transcription factors, cis-acting elements directly participate in gene expression regulation (**Supplementary Fig. 3**).

We detected 23 elements associated with biological functions, and they were divided into four categories: Plant hormone-responsive, abiotic stress-responsive, plant growth and development-related, and light-responsive ele-

Table 1. Classification of cis-acting elements in *AsNRT1s*.

Cis-regulatory element	Element	Element number	Classification
Abscisic acid responsiveness	ABRE	644	Hormone response related elements
Flavonoid biosynthetic genes regulation	MBSI	14	Hormone response related elements
Auxin-responsive element	AuxRE, TGA-box, TGA-element	175	Hormone response related elements
Gibberellin-responsiveness	GARE-motif, P-box, TATC-box	175	Hormone response related elements
Salicylic acid responsiveness	SARE, TCA-element	95	Hormone response related elements
The MeJA-responsiveness	CGTCA-motif, TGACG-motif	450	Hormone response related elements
Defense and stress responsiveness	TC-rich repeats	54	Abiotic stress response element
Drought-inducibility	MBS	182	Abiotic stress response element
Low-temperature responsiveness	LTR	155	Abiotic stress response element
Maximal elicitor-mediated activation (2 copies)	AT-rich sequence	6	Abiotic stress response element
MYBHv1 binding site	CCAAT-box	136	Abiotic stress response element
Wound-responsive element	WUN-motif	4	Abiotic stress response element
Endosperm expression	GCN4-motif	40	Plant growth and development elements
Endosperm-specific negative expression	AACA-motif	5	Plant growth and development elements
Anoxic specific inducibility	GC-motif	106	Plant growth and development elements
Differentiation of the palisade mesophyll cells	HD-Zip 1	16	Plant growth and development elements
Essential for the anaerobic induction	ARE	307	Plant growth and development elements
Meristem expression	CAT-box	175	Plant growth and development elements
Meristem specific activation	NON-box	2	Plant growth and development elements
Root specific	motif I	9	Plant growth and development elements
Seed-specific regulation	RY	32	Plant growth and development elements
Zein metabolism regulation	O2-site-a	122	Plant growth and development elements
Light responsive element	I-box, Gap-box, Box II, L-box	1883	Elements associated with light response

MeJA, methyl jasmonate; MBS, MYB binding sites; ABRE, abscisic acid responsive element; MBSI, MYB binding Site I; AuxRE, auxin response element; SARE, salicylic acid responsive element; LTR, low temperature response; ARE, antioxidant response element; WUN, wound-responsive element; GCN4, general control nonderepressible 4.

ments (Table 1). In addition, we detected ten elements associated with plant growth and development. These elements comprised GCN4_motif (related to endosperm expression), AACA_motif (specifically regulated by endosperm), GC-motif (related to hypoxia induction), HD-Zip 1 motif (related to palisade mesophyll cell differentiation), cis elements involved in anaerobic induction response, CAT-box (related to meristematic expression), NON-box (activated by meristematic tissue), root-specific expression motif I, RY-motif (regulated by seed specificity), and O2-site-a (regulated by zein metabolism). Among them, anaerobic induction-related elements were the most abundant functional components.

Furthermore, we detected six elements related to plant stress response, including TC-rich repeat sequences (related to defense and stress response), MYB binding sites (MBS)-elements (related to drought induction), LTR elements (related to low temperature response), MYBHv1 binding site (CCAAT-box), and WUN-motifs (related to wound response). These elements play key regulatory roles in plant development and environmental stress response. In addition, we detected six cis-sacting elements related to hormone response, including abscisic acid-responsive ABRE-element (related to abscisic acid), flavonoid biosynthesis-regulated MBSI-motif (related to MYB transcription factor-mediated regulation of flavonoid synthesis gene expression), auxin-responsive AuxRE-element (related to growth and development regulated by growth hormone) and TGA-box/TGA-motif (related to plant disease resistance response), gibberellin-responsive GARE-motif/P-box/TACT-box (related to gibberellin signaling pathway), salicylic acid-responsive SARE-element/TCA-motif (related to plant disease resistance response and abiotic stress response), and methyl jasmonate (MeJA)-responsive CGTCA-motif/TGACG-motif (related to plant defense responses and secondary metabolism). These components recognize specific stress signals within cells and mediate the regulation of related gene expression to adapt to unfavorable external environments. Further, we identified I-box, Gap-box, Box-II, and L-box components related to light response. Overall, the identified cis-acting elements were related to the response mechanisms of plants to internal hormone signals, external environmental stress, and the expression regulation patterns in specific growth stages and tissues, indicating that the *AsNRT1* family might be involved in regulating multidimensional biological processes in oat.

3.7 Tissue Expression Specificity Analysis of the AsNRT1 Family

By comparing the gene expression data of diploid *A. longigluis* and hexaploid *A. sativa*, the expression patterns of the *AsNRT1* family in different tissues were analyzed, and their potential biological functions were explored. A total of 114 gene replication pairs were identified (Fig. 2). The expression data for these diploid oat genes were obtained from the oat database, and a tissue-specific expression heat map was drawn (Fig. 4). The expression levels of the *AsNRT1s* varied across different tissues. Most *AsNRT1s* exhibited tissue-specific expression, with distinct patterns observed for key members. *AsNPF4.18* was highly expressed in the root tip, potentially mediating the initial uptake of nitrate by the root system. *AsNPF7.16*, *AsNPF7.19*, and *AsNPF2.6* were highly expressed in the roots, potentially mediating nitrate uptake from the soil to the root system, intra-root transport, and xylem loading. *AsNPF4.5*, *AsNPF2.7*, and *AsNPF6.8* were highly expressed in the leaves, potentially acting as unloading/loading hubs for vascular transport and, at the same time, participating in nitrogen signaling to coordinate metabolism and growth. *AsNPF2.1* and *AsNPF6.13* were highly expressed in the panicles and might mediate nitrate partitioning from the nutrient organs to inflorescences or act as signaling elements. *AsNPF6.2* was highly expressed in the spikelets, potentially supplying nitrogen to the spikelets via the "source-deposit" transporter network to support floral organ development, pollen viability, and seed formation. Therefore, nitrogen uptake in oat might be initiated by *AsNPF6.1* and *AsNPF6.3*, which take up nitrate from the soil. This process is followed by the activities of *AsNPF7.16*, *AsNPF7.19*, and *AsNPF2.6* that mediate intra-root nitrate transport. Next, vascular nitrate transport is mediated by *AsNPF4.5*, *AsNPF2.7*, and *AsNPF6.8*, and *AsNPF2.1* and *AsNPF6.13* mediated nitrate partitioning to the florets. Finally, precise nitrogen transport to the spikelets was facilitated by *AsNPF6.2* to mediate seed formation.

3.8 Expression Analysis of the Nitrogen-Responsive AsNRT1s

We selected 10 genes from the promoter region containing many adversity-related cis-acting elements to validate the bioinformatics data related to the expression analysis of oat *NPFs*. The genes showing large differences in their expressions across different tissues were found to be involved in nitrate uptake and transport in other plants. These genes were homologous with *AsNPF6.2*, *AsNPF4.5*, *AsNPF2.1*, *AsNPF6.8*, *AsNPF4.18*, *AsNPF2.6*, *AsNPF2.7*, *AsNPF7.16*, *AsNPF7.19*, and *AsNPF6.13*.

To verify the expression patterns of these ten genes under LN conditions in oats, we created a CK group (treated with 20 mM nitrogen) and an LN group (treated with 2 mM nitrogen) and analyzed the expressions of these genes in their root and leaf tissues. Our results showed that under

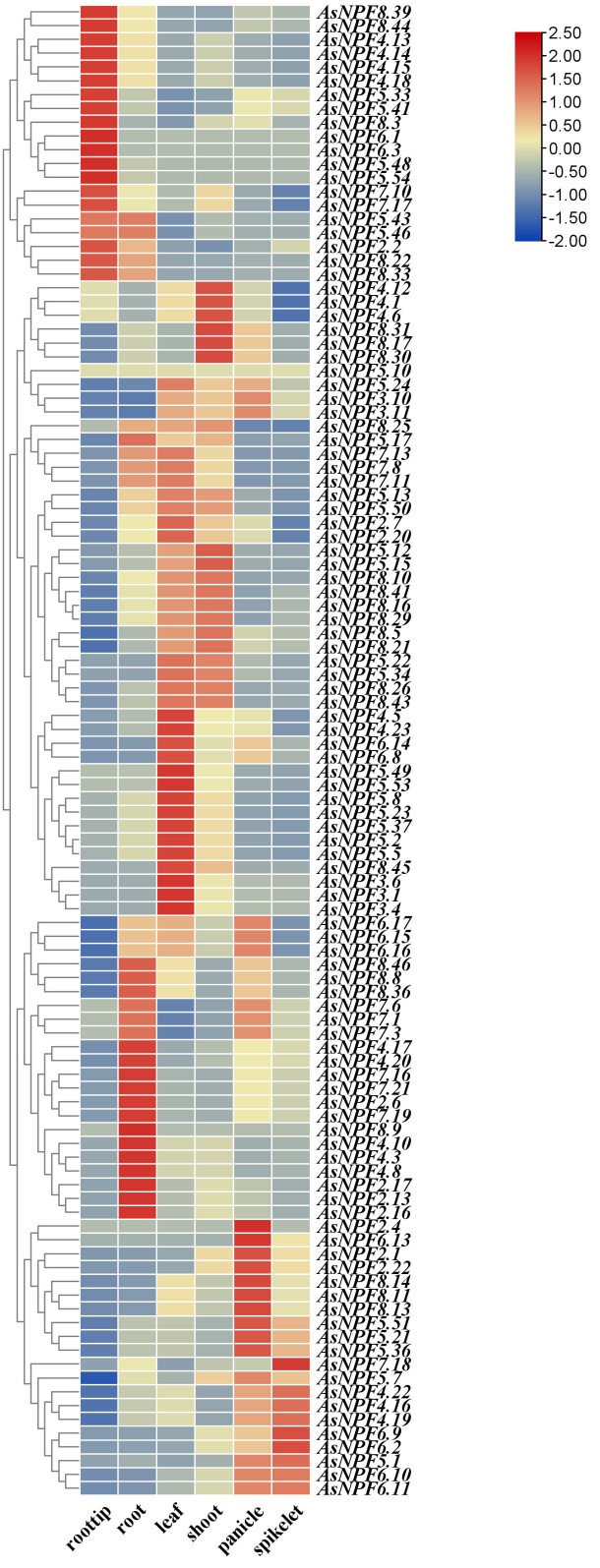

Fig. 4. Heat map of the expression profiles of *AsNRT1s* in different tissues. From left to right are the root tip, root, leaf, shoot, panicle, and spikelet. Orange and blue represent high and low expressions, respectively.

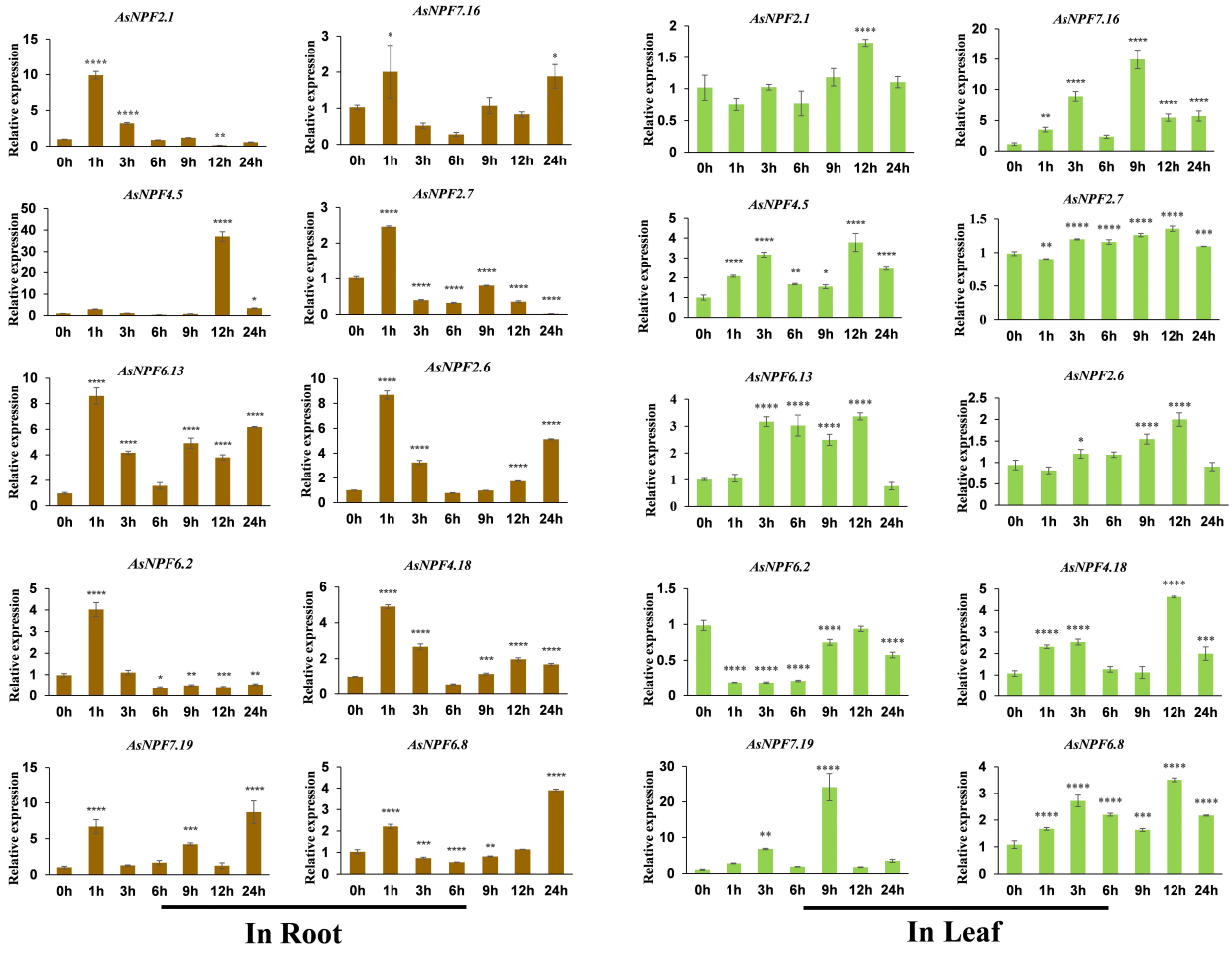

Fig. 5. The left and right figures show the expression profile of ten *AsNRT1s* in oat root and leaf tissue under low nitrogen (LN) treatment, respectively. The data is standardized using the *actin* gene as an internal reference, and the vertical error line represents the standard deviation (SD). Asterisks indicate significant differences in gene expression compared to the untreated control group (Student's *t*-test: * $p < 0.05$, ** $p < 0.01$, *** $p < 0.001$, **** $p < 0.0001$), with the number of asterisks reflecting different levels of significance.

LN conditions, the expressions of these genes were induced to varying degrees. In the roots of the LN group (Fig. 5), the levels of 8 of these 10 genes were significantly higher at 1 h post-treatment than those at 0 h ($p < 0.01$). Then, the expressions of *AsNPF7.16*, *AsNPF6.13*, *AsNPF2.6*, *AsNPF4.18*, *AsNPF7.19*, and *AsNPF6.8* first decreased and then increased over time, with significantly higher levels at 24 h than at 0 h ($p < 0.05$). In contrast, the expressions of *AsNPF2.1*, *AsNPF2.7* and *AsNPF6.2* declined over time, with significantly lower levels at 24 h than at 0 h ($p < 0.05$). The expression of *AsNPF4.5* peaked at 12 h post-treatment, being significantly higher than that at 0 h ($p < 0.01$). These results indicated that *AsNPF7.16*, *AsNPF6.13*, *AsNPF2.6*, *AsNPF4.18*, *AsNPF7.19*, and *AsNPF6.8* are potential nitrogen-responsive genes in oat leaves.

Unlike the gene expression pattern in root tissue, the expression of *AsNPF2.1* exhibited specific regulatory characteristics in leaf tissue under LN treatment (Fig. 5). At 12 h post-treatment, its levels were significantly higher than at 0 h ($p < 0.01$). However, its levels at any other time points were not significantly different than those at 0 h. Furthermore, the levels of *AsNPF7.16*, *AsNFP4.5*, *AsNPF2.7*, *AsNPF6.13*, *AsNPF2.6*, *AsNPF4.18*, and *AsNPF6.8* were significantly higher compared to those at 0 h ($p < 0.05$) and all the genes exhibited a similar expression pattern. On the other hand, *AsNPF6.2* showed a decreasing trend, exhibiting significantly lower levels at almost all time points compared to its levels at 0 h ($p < 0.01$). Furthermore, compared to its levels at 0 h, the *AsNPF7.19* expression significantly increased at 3 h and 9 h ($p < 0.01$). These results indicated that all the assessed genes might act as potential LN treatment-responsive genes in root tissues except for *AsNPF6.2*. We selected *AsNPF2.6*, *AsNPF4.5*, *AsNPF6.8*, *AsNPF7.16*, and *AsNPF7.19* for subsequent qRT-PCR analysis.

3.9 Subcellular Localization Analysis of Oat AsNRT1 Family

Next, we analyzed the subcellular localization of candidate proteins encoded by the *AsNRT1s*. Analysis using

the wheat protoplast expression system showed that the GFP signal was distributed in the cytoplasm and cell membrane of wheat protoplasts (Fig. 6). Among them, weak GFP signals in the cytoplasm and cell membrane were observed only for *AsNPF2.6* and *AsNPF4.5*. *AsNPF6.8, AsNPF7.16*, and *AsNPF7.19* exhibited stronger GFP signals in the cytoplasm but weaker signals in the cell membrane. This finding was not in line with the biological prediction. These findings indicated that these 5 genes might primarily be involved in nitrogen transport and uptake in the oat cytoplasm and cell membrane.

4. Discussion

The *NRT1* family comprises critical genes involved in plant nitrogen uptake and utilization, and its members are engaged in nitrate transport and uptake. A study has shown that nitrate uptake and translocation are influenced by numerous factors, with light being a critical factor [23]. Bioinformatic analysis of the promoters of 197 *AsNRT1s* revealed that they contain abundant plant hormone and stress-responsive regulatory elements. The hormone-responsive elements were related to various hormone-related signaling pathways, such as gibberellin (GA)-, abscisic acid (ABA)-, auxin (IAA)-, MeJA-, and salicylic acid (SA)-related signaling pathways. Stress-responsive elements included drought-induced MBS, while environmental factors-responsive components comprised light-responsive regulatory components. Notably, among all the identified regulatory elements, the most abundant were the photoresponsive cis-acting elements (39.3%). This predominance might reflect photoperiod-driven metabolic coordination, where photosynthetic product accumulation creates elevated nitrogen demands for biomass synthesis. The abundance of these light-sensitive elements suggested their critical role in mediating plant–environment interactions via transcriptional regulation of nutrient acquisition pathways. This result was consistent with the genome-wide analysis of the *NRT1* family promoters in grains [42]. In addition to photoresponsive elements, oat *NRT1s* were also regulated via multiple hormone signaling pathways. This finding was consistent with the results of previous studies. For instance, previous study [47] has shown that hormones significantly regulate the expression of cotton *GhNPF* family. In *Arabidopsis thaliana*, *AtNRT1.1* transports growth hormone in lateral roots and responds to nitrogen starvation by inhibiting lateral root growth [48]. Cytokinins positively regulate the expression of *AtNRT1.4* and *AtNRT1.7*, promoting nitrate distribution and transport [17,20]. In the present study, analysis of hormone-responsive cis-elements revealed distinct regulatory signatures. ABA-responsive motifs constituted 13.5% of the identified elements, while MeJA-responsive elements constituted 9.4%. This finding indicated a strong functional linkage between *NRT1* expression dynamics and phytohormone signaling pathways, particularly suggesting that ABA and MeJA mediated transcriptional regulation of nitrate transport processes. These results showed that the expression of *AsNRT1s* might be regulated by various plant hormones and environmental factors, thereby reflecting the functional diversity of this gene family.

The function of a gene is based on its expression, while the expression of a gene reflects its function [49]. We analyzed the tissue-specific expression patterns of 197 *AsNRT1s*. The seed- and spike-specific expressions of *TaNPF1* in wheat have been shown to be related to its nitrate transport function during seed development [50]. The *AsNRT1* family exhibited diverse tissue expression specificity. *AsNPF6.1* and *AsNPF6.3* exhibited preferentially high expression in the root tip, *AsNPF8.9* was specifically upregulated in mature roots, and *AsNPF2.4* displayed panicle-specific expression. These findings suggested that these genes might function predominantly in specific tissues to regulate nitrate transport and localized nitrogen metabolism. On the contrary, multiple *AsNRT1* family members, including *AsNPF2.20*, *AsNPF6.2*, and *AsNPF6.17*, exhibited constitutive expression in various tissues, suggesting their potential involvement in the systemic nitrogen regulation during oat growth and development.

Under LN conditions, *AtNRT1.1* (*AtNPF6.3*) exhibited opposite expression patterns in aboveground tissues and roots, suggesting varied regulatory mechanisms for *AtNPF6.3* in these tissue types [2]. Previous studies on the maize homologous gene, *ZmNPF6.6*, reported similar results under LN conditions, showing opposite expression trends in the roots and leaves under LN treatment [45,51]. The homologous gene in wheat, *TaNPF6.3-6D*, was significantly upregulated in the roots at 6 h and peaked at 24 h under LN treatment, but it exhibited an opposite expression pattern in the leaves [52,53]. In the current study, under LN treatment, *AsNPF6.2*, *AsNPF2.7*, and *AsNPF2.6* were first upregulated and then downregulated in the leaves, and first downregulated and then upregulated in the roots, indicating potential inhibitory effects of these genes on the nitrate uptake system [54]. These results indicated that *AsNPF6.2*, *AsNPF2.7*, and *AsNPF2.6* exhibited opposite expression patterns in roots and leaves under LN treatment, which was in line with the findings in other species. This finding suggested that these oat genes might also play similar functions and roles as their corresponding genes in other species. Among them, the expressions of *AsNPF7.16* and *AsNPF7.19* were significantly higher in the roots than in other tissues, suggesting that they might play an important role in nitrate transport and uptake in the roots. In contrast, the expression of *AsNPF4.5* was significantly higher in the leaves than in the roots.

The functional characteristics, metabolic activity, and interaction patterns of proteins are closely related to their subcellular localization. The functions of proteins vary based on their location within the cells. This implies that proteins must be present in specific subcellular structures

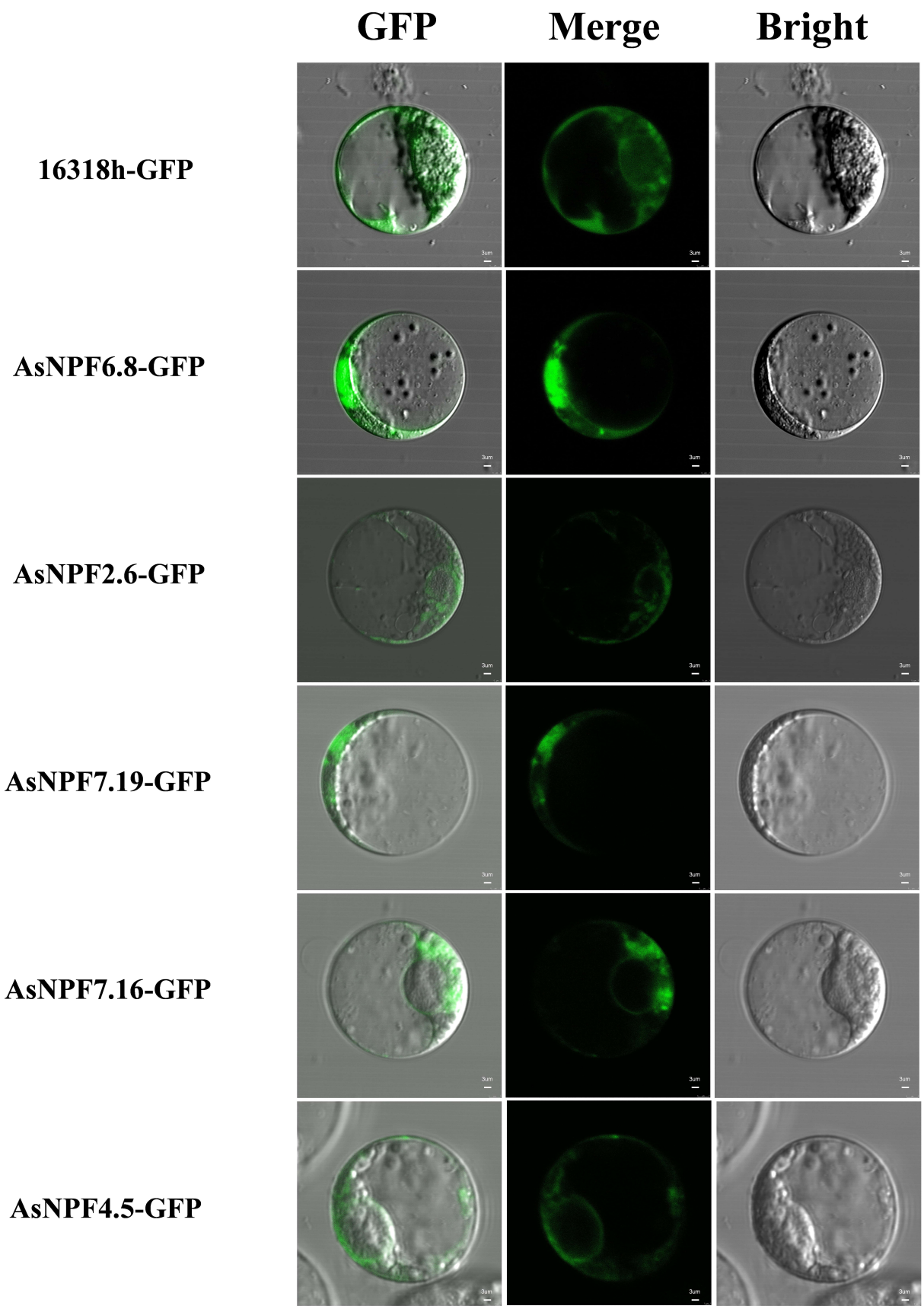

Fig. 6. Subcellular localization of *AsNRT1s*. Green fluorescent protein (GFP) stands for green fluorescence field, merge stands for superimposed field, and bright stands for bright field. GFP field: 488 nm. Scale bars = 3 μm.

to fulfill their biological functions. Thus, subcellular localization analysis of proteins is crucial to studying their functions. In *Arabidopsis thaliana*, *AtNPF5.12* and *AtNPF5.16* are located on the vesicle membrane and participate in the long-distance transport of nitrate from the root system to the aboveground tissues [55]. There are two splicing variants of *OsNPF7.7* in rice, *OsNPF7.7-1* and *OsNPF7.7-2*. Among them, *OsNPF7.7-1* is located on the cell membrane, and its upregulation can promote nitrate absorption in the roots [56]. As a functionally homologous protein of *Arabidopsis thaliana* *AtNPF6.3* (*NRT1.1/CHL1*), rice *OsNPF6.5* is also located on the cell membrane, and its expression is significantly upregulated by nitrate induction [44]. There are subcellular localization differences between the tandem repeat genes *ZmNRT1.1B* and *ZmNRT1.1C* in maize. *ZmNRT1.1B* is located on the plasma membrane, while the fluorescence signals from ZmNRT1.1C-GFP fusion protein are distributed in the inner membrane-like structure, suggesting that these two protein subtypes might exhibit different functions [51]. In the present study, *AsNPF4.5*, *AsNPF6.8*, *AsNPF2.6*, *AsNPF7.16*, and *AsNPF7.19* were transferred into the 16318h-GFP vector and transformed into wheat protoplasts using a seamless cloning method. Laser confocal microscopy revealed that these genes were predominantly present in the cytoplasm and cell membrane of the protoplasts. Among them, the *AsNPF2.6* and *AsNPF4.5* signals were weak in the cytoplasm. We observed strong *AsNPF6.8*, *AsNPF7.16*, and *AsNPF7.19* signals in the cytoplasm but weak signals on the cell membrane. The localization paterns of these genes were different from those of *NRT1s* in other species. Therefore, we speculated that *NRT1.1*, which is partially distributed in the cytoplasm due to functional redundancy in leaf epidermal cells or in seedling-stage leaf cells, might be transiently retained in the cytoplasm due to the immature membrane transport system, while it becomes stably localized in the plasma membrane during the maturation stage [57]. We also speculated that deletions or missense mutations (for example, α-helix$\rightarrow$ β-folding) in the transmembrane regions (such as transmembrane helices 4, 7, and 11) in the *NRT1* family members might prevent the proteins from entering the membrane structure, leading to their retention in the cytoplasm [18].

5. Conclusions

Here, we performed a genome-wide characterization of the oat *NRT1* family. A total of 197 *AsNRT1* family members were identified, which were divided into 8 subfamilies based on their evolutionary relationships, with the members in the same subfamily exhibiting similar gene structures and conserved motifs. A comprehensive analysis of the chromosomal location, gene structure, and cis-acting elements of the 197 *AsNRT1s* showed that the oat *NRT1s* are involved in a coordinated response to adverse conditions and phytohormones. We further analyzed the expressions of ten candidate genes under LN treatment using qRT-PCR and found that five key oat *NRT1s* were induced by nitrogen treatment. Finally, the locations of the proteins encoded by these 5 *NRT1s* were identified as the cytoplasm and cell membrane by gene cloning and subcellular localization analyses. Our findings provided valuable information for further functional validation and laid a theoretical foundation for molecular breeding for optimal oat production.

Abbreviations

CK, control; GRAVY, grand average of hydropathy; LN, low nitrogen; MW, molecular weight; NRT1, nitrate transporter 1; pI, isoelectric point.

Availability of Data and Materials

All data generated or analyzed during this study are included in this published article and its supplementary information files.

Author Contributions

RC and QX conceived the project. WZheng and SQG designed the experiments. RC and QX performed most of the experiments with the help of JG, RWS, YKD and WZhao. RC, SQG and JG analyzed the data and wrote the article. All authors contributed to editorial changes in the manuscript. All authors read and approved the final manuscript. All authors have participated sufficiently in the work and agreed to be accountable for all aspects of the work.

Ethics Approval and Consent to Participate

Prof. Zhao Guiqin of Gansu Agricultural University provided and agreed to use Baiyan VII as experimental material for the experiment.

Acknowledgment

Not applicable.

Funding

This study was supported by the National Key Research and Development Program “Assessment of Carrying Capacity of Important Grassland Animal Husbandry and Potential for Ecological Animal Husbandry Base Construction in Xinjiang” (2022xjkk0404), “Integration of Highly Efficient Biological Breeding Technological Innovations and Application of Breakthrough Variety Breeding in Wheat” (KJCX20251004), Creation of new transgenic germplasm of important crops (KJCX20230203, KJCX20240305), Beijing Nova Program (20250484810) and National Natural Science Foundation of China’s “Research on Nitrogen Utilization Efficiency and Quality Improvement under the Mechanism of Root and Soil Action of Intercropping of Legume Forage and Kurrer’s Xiangshi Pear” (32060402).

Conflict of Interest

The authors declare no conflict of interest.

Supplementary Material

Supplementary material associated with this article can be found, in the online version, at https://doi.org/10.31083/FBL39679.

References

[1] Kusano M, Fukushima A, Redestig H, Saito K. Metabolomic approaches toward understanding nitrogen metabolism in plants. Journal of Experimental Botany. 2011; 62: 1439–1453. https://doi.org/10.1093/jxb/erq417.

[2] Sakuraba Y, Chaganzhana, Mabuchi A, Iba K, Yanagisawa S. Enhanced NRT1.1/NPF6.3 expression in shoots improves growth under nitrogen deficiency stress in Arabidopsis. Communications Biology. 2021; 4: 256. https://doi.org/10.1038/s42003-021-01775-1.

[3] Pan Z, He P, Fan D, Jiang R, Song D, Song L, *et al*. Global impact of enhanced-efficiency fertilizers on vegetable productivity and reactive nitrogen losses. The Science of the Total Environment. 2024; 926: 172016. https://doi.org/10.1016/j.scitotenv.2024.172016.

[4] Itin-Shwartz B. Survey based Assessment of Sustainable Agricultural Practices: Evidence from Indian Plots. Agribusiness. 2024; 40: 416–457. https://doi.org/10.1002/agr.21890.

[5] Caires EF, Bini AR, Duart VM, Ricardo KS, Alves LM. Co-inoculation of Azospirillum brasilense and late nitrogen fertilization for no-till soybean production. Agronomy Journal. 2024; 116: 2034–2047. https://doi.org/10.1002/agj2.21602.

[6] Liu J, You L, Amini M, Obersteiner M, Herrero M, Zehnder AJB, *et al*. A high-resolution assessment on global nitrogen flows in cropland. Proceedings of the National Academy of Sciences of the United States of America. 2010; 107: 8035–8040. https://doi.org/10.1073/pnas.0913658107.

[7] Coskun D, Britto DT, Shi W, Kronzucker HJ. Nitrogen transformations in modern agriculture and the role of biological nitrification inhibition. Nature Plants. 2017; 3: 17074. https://doi.org/10.1038/nplants.2017.74.

[8] Guo JH, Liu XJ, Zhang Y, Shen JL, Han WX, Zhang WF, *et al*. Significant acidification in major Chinese croplands. Science (New York, N.Y.). 2010; 327: 1008–1010. https://doi.org/10.1126/science.1182570.

[9] Robertson GP, Vitousek PM. Nitrogen in Agriculture: Balancing the Cost of an Essential Resource. Annual Review of Environment and Resources. 2009; 34: 97–125. http://dx.doi.org/10.1146/annurev.environ.032108.105046.

[10] Lezhneva L, Kiba T, Feria-Bourrellier AB, Lafouge F, Boutet-Mercey S, Zoufan P, *et al*. The Arabidopsis nitrate transporter NRT2.5 plays a role in nitrate acquisition and remobilization in nitrogen-starved plants. The Plant Journal: for Cell and Molecular Biology. 2014; 80: 230–241. https://doi.org/10.1111/tpj.12626.

[11] Walch-Liu P, Forde BG. Nitrate signalling mediated by the NRT1.1 nitrate transporter antagonises L-glutamate-induced changes in root architecture. The Plant Journal: for Cell and Molecular Biology. 2008; 54: 820–828. https://doi.org/10.1111/j.1365-313X.2008.03443.x.

[12] Léran S, Varala K, Boyer JC, Chiurazzi M, Crawford N, Daniel-Vedele F, *et al*. A unified nomenclature of NITRATE TRANSPORTER 1/PEPTIDE TRANSPORTER family members in plants. Trends in Plant Science. 2014; 19: 5–9. https://doi.org/10.1016/j.tplants.2013.08.008.

[13] Tsay YF, Chiu CC, Tsai CB, Ho CH, Hsu PK. Nitrate transporters and peptide transporters. FEBS Letters. 2007; 581: 2290–2300. https://doi.org/10.1016/j.febslet.2007.04.047.

[14] Huang NC, Liu KH, Lo HJ, Tsay YF. Cloning and functional characterization of an Arabidopsis nitrate transporter gene that encodes a constitutive component of low-affinity uptake. The Plant Cell. 1999; 11: 1381–1392. https://doi.org/10.1105/tpc.11.8.1381.

[15] Wang W, Hu B, Li A, Chu C. NRT1.1s in plants: functions beyond nitrate transport. Journal of Experimental Botany. 2020; 71: 4373–4379. https://doi.org/10.1093/jxb/erz554.

[16] Liu KH, Huang CY, Tsay YF. CHL1 is a dual-affinity nitrate transporter of Arabidopsis involved in multiple phases of nitrate uptake. The Plant Cell. 1999; 11: 865–874. https://doi.org/10.1105/tpc.11.5.865.

[17] Chiu CC, Lin CS, Hsia AP, Su RC, Lin HL, Tsay YF. Mutation of a nitrate transporter, AtNRT1:4, results in a reduced petiole nitrate content and altered leaf development. Plant & Cell Physiology. 2004; 45: 1139–1148. https://doi.org/10.1093/pcp/pch143.

[18] Lin SH, Kuo HF, Canivenc G, Lin CS, Lepetit M, Hsu PK, *et al*. Mutation of the Arabidopsis NRT1.5 nitrate transporter causes defective root-to-shoot nitrate transport. The Plant Cell. 2008; 20: 2514–2528. https://doi.org/10.1105/tpc.108.060244.

[19] Almagro A, Lin SH, Tsay YF. Characterization of the Arabidopsis nitrate transporter NRT1.6 reveals a role of nitrate in early embryo development. The Plant Cell. 2008; 20: 3289–3299. https://doi.org/10.1105/tpc.107.056788.

[20] Fan SC, Lin CS, Hsu PK, Lin SH, Tsay YF. The Arabidopsis nitrate transporter NRT1.7, expressed in phloem, is responsible for source-to-sink remobilization of nitrate. The Plant Cell. 2009; 21: 2750–2761. https://doi.org/10.1105/tpc.109.067603.

[21] Tian H, Yuan X, Duan J, Li W, Zhai B, Gao Y. Influence of nutrient signals and carbon allocation on the expression of phosphate and nitrogen transporter genes in winter wheat (Triticum aestivum L.) roots colonized by arbuscular mycorrhizal fungi. PloS One. 2017; 12: e0172154. https://doi.org/10.1371/journal.pone.0172154.

[22] Araújo OJL, Pinto MS, Sperandio MVL, Santos LA, Stark EMLM, Fernandes MS, *et al*. Expression of the Genes OsNRT1.1, OsNRT2.1, OsNRT2.2, and Kinetics of Nitrate Uptake in Genetically Contrasting Rice Varieties. American Journal of Plant Sciences. 2015; 6: 306–314. https://doi.org/10.4236/ajps.2015.62035.

[23] Duan W, Wang S, Zhang H, Xie B, Zhang L. Plant growth and nitrate absorption and assimilation of two sweet potato cultivars with different N tolerances in response to nitrate supply. Scientific Reports. 2024; 14: 21286. https://doi.org/10.1038/s41598-024-72422-y.

[24] Qiao Y, Zhao L, Gao D, Zhang L, Guo L, Ge J, *et al*. Study on Optimal Nitrogen Application for Different Oat Varieties in Dryland Regions of the Loess Plateau. Plants (Basel, Switzerland). 2024; 13: 2956. https://doi.org/10.3390/plants13212956.

[25] Martinez MF, Arelovich HM, Wehrhahne LN. Grain yield, nutrient content and lipid profile of oat genotypes grown in a semi-arid environment. Field Crops Research. 2009; 116: 92–100. https://doi.org/10.1016/j.fcr.2009.11.018.

[26] Read JJ, Reddy KR, Jenkins JN. Yield and fiber quality of Upland cotton as influenced by nitrogen and potassium nutrition. European Journal of Agronomy. 2005; 24: 282–290. https://doi.org/10.1016/j.eja.2005.10.004.

[27] Peng Y, Yan H, Guo L, Deng C, Wang C, Wang Y, *et al*. Reference genome assemblies reveal the origin and evolution of allohexaploid oat. Nature Genetics. 2022; 54: 1248–1258. https://doi.org/10.1038/s41588-022-01127-7.

[28] Bolser DM, Staines DM, Perry E, Kersey PJ. Ensembl Plants: Integrating Tools for Visualizing, Mining, and Analyzing Plant Genomic Data. Methods in Molecular Biology

(Clifton, N.J.). 2017; 1533: 1–31. https://doi.org/10.1007/978-1-4939-6658-5_1.
[29] Mistry J, Chuguransky S, Williams L, Qureshi M, Salazar GA, Sonnhammer ELL, *et al*. Pfam: The protein families database in 2021. Nucleic Acids Research. 2021; 49: D412–D419. https://doi.org/10.1093/nar/gkaa913.
[30] Finn RD, Clements J, Eddy SR. HMMER web server: interactive sequence similarity searching. Nucleic Acids Research. 2011; 39: W29–W37. https://doi.org/10.1093/nar/gkr367.
[31] Yang M, Derbyshire MK, Yamashita RA, Marchler-Bauer A. NCBI's Conserved Domain Database and Tools for Protein Domain Analysis. Current Protocols in Bioinformatics. 2020; 69: e90. https://doi.org/10.1002/cpbi.90.
[32] Duvaud S, Gabella C, Lisacek F, Stockinger H, Ioannidis V, Durinx C. Expasy, the Swiss Bioinformatics Resource Portal, as designed by its users. Nucleic Acids Research. 2021; 49: W216–W227. https://doi.org/10.1093/nar/gkab225.
[33] Horton P, Park KJ, Obayashi T, Fujita N, Harada H, Adams-Collier CJ, *et al*. WoLF PSORT: protein localization predictor. Nucleic Acids Research. 2007; 35: W585–W587. https://doi.org/10.1093/nar/gkm259.
[34] Chou KC, Shen HB. Plant-mPLoc: a top-down strategy to augment the power for predicting plant protein subcellular localization. PloS One. 2010; 5: e11335. https://doi.org/10.1371/journal.pone.0011335.
[35] Kumar S, Stecher G, Li M, Knyaz C, Tamura K. MEGA X: Molecular Evolutionary Genetics Analysis across Computing Platforms. Molecular Biology and Evolution. 2018; 35: 1547–1549. https://doi.org/10.1093/molbev/msy096.
[36] Subramanian B, Gao S, Lercher MJ, Hu S, Chen WH. Evolview v3: a webserver for visualization, annotation, and management of phylogenetic trees. Nucleic Acids Research. 2019; 47: W270–W275. https://doi.org/10.1093/nar/gkz357.
[37] Chen C, Chen H, Zhang Y, Thomas HR, Frank MH, He Y, *et al*. TBtools: An Integrative Toolkit Developed for Interactive Analyses of Big Biological Data. Molecular Plant. 2020; 13: 1194–1202. https://doi.org/10.1016/j.molp.2020.06.009.
[38] Bailey TL, Boden M, Buske FA, Frith M, Grant CE, Clementi L, *et al*. MEME SUITE: tools for motif discovery and searching. Nucleic Acids Research. 2009; 37: W202–W208. https://doi.org/10.1093/nar/gkp335.
[39] Lescot M, Déhais P, Thijs G, Marchal K, Moreau Y, Van de Peer Y, *et al*. PlantCARE, a database of plant cis-acting regulatory elements and a portal to tools for in silico analysis of promoter sequences. Nucleic Acids Research. 2002; 30: 325–327. https://doi.org/10.1093/nar/30.1.325.
[40] Teste, MA, Duquenne, M, François, JM, Parrou, JL. Validation of reference genes for quantitative expression analysis by real-time RT-PCR in Saccharomyces cerevisiae. BMC molecular biology. 2009; 10: 99. https://doi.org/10.1186/1471-2199-10-99.
[41] Wilson S, Dagvadorj B, Tam R, Schwessinger B. Wheat Protoplast Preparation and Transformation. protocols.io. 2023. https://doi.org/10.17504/protocols.io.q26g7r3zkvwz/v1.
[42] Cheng J, Tan H, Shan M, Duan M, Ye L, Yang Y, *et al*. Genome-wide identification and characterization of the NPF genes provide new insight into low nitrogen tolerance in *Setaria*. Frontiers in Plant Science. 2022; 13: 1043832. https://doi.org/10.3389/fpls.2022.1043832.
[43] Léran S, Muños S, Brachet C, Tillard P, Gojon A, Lacombe B. Arabidopsis NRT1.1 is a bidirectional transporter involved in root-to-shoot nitrate translocation. Molecular Plant. 2013; 6: 1984–1987. https://doi.org/10.1093/mp/sst068.
[44] Hu B, Wang W, Ou S, Tang J, Li H, Che R, *et al*. Variation in NRT1.1B contributes to nitrate-use divergence between rice subspecies. Nature Genetics. 2015; 47: 834–838. https://doi.org/10.1038/ng.3337.
[45] Wen Z, Tyerman SD, Dechorgnat J, Ovchinnikova E, Dhugga KS, Kaiser BN. Maize NPF6 Proteins Are Homologs of Arabidopsis CHL1 That Are Selective for Both Nitrate and Chloride. The Plant Cell. 2017; 29: 2581–2596. https://doi.org/10.1105/tpc.16.00724.
[46] Holub EB. The arms race is ancient history in Arabidopsis, the wildflower. Nature Reviews. Genetics. 2001; 2: 516–527. https://doi.org/10.1038/35080508.
[47] Liu J, Wang C, Peng J, Ju J, Li Y, Li C, *et al*. Genome-wide investigation and expression profiles of the *NPF* gene family provide insight into the abiotic stress resistance of *Gossypium hirsutum*. Frontiers in Plant Science. 2023; 14: 1103340. https://doi.org/10.3389/fpls.2023.1103340.
[48] Chiba Y, Shimizu T, Miyakawa S, Kanno Y, Koshiba T, Kamiya Y, *et al*. Identification of Arabidopsis thaliana NRT1/PTR FAMILY (NPF) proteins capable of transporting plant hormones. Journal of Plant Research. 2015; 128: 679–686. https://doi.org/10.1007/s10265-015-0710-2.
[49] Zhu T, Liu Y, Ma L, Wang X, Zhang D, Han Y, *et al*. Genome-wide identification, phylogeny and expression analysis of the SPL gene family in wheat. BMC Plant Biology. 2020; 20: 420. https://doi.org/10.1186/s12870-020-02576-0.
[50] Kumar A, Sandhu N, Kumar P, Pruthi G, Singh J, Kaur S, *et al*. Genome-wide identification and in silico analysis of NPF, NRT2, CLC and SLAC1/SLAH nitrate transporters in hexaploid wheat (Triticum aestivum). Scientific Reports. 2022; 12: 11227. https://doi.org/10.1038/s41598-022-15202-w.
[51] Cao H, Liu Z, Guo J, Jia Z, Shi Y, Kang K, *et al*. ZmNRT1.1B (ZmNPF6.6) determines nitrogen use efficiency via regulation of nitrate transport and signalling in maize. Plant Biotechnology Journal. 2024; 22: 316–329. https://doi.org/10.1111/pbi.14185.
[52] Li Q, Song HL, Zhou T, Pei MN, Wang B, Yan SX, *et al*. Differential Morpho-Physiological, Ionomic, and Phytohormone Profiles, and Genome-Wide Expression Profiling Involving the Tolerance of Allohexaploid Wheat (*Triticum aestivum* L.) to Nitrogen Limitation. Journal of Agricultural and Food Chemistry. 2024; 72: 3814–3831. https://doi.org/10.1021/acs.jafc.3c08626.
[53] Meng X, Lou H, Zhai S, Zhang R, Liu G, Xu W, *et al*. TaNAM-6A is essential for nitrogen remobilisation and regulates grain protein content in wheat (Triticum aestivum L.). Plant, Cell & Environment. 2024; 47: 2310–2321. https://doi.org/10.1111/pce.14878.
[54] Filleur S, Daniel-Vedele F. Expression analysis of a high-affinity nitrate transporter isolated from Arabidopsis thaliana by differential display. Planta. 1999; 207: 461–469. https://doi.org/10.1007/s004250050505.
[55] He YN, Peng JS, Cai Y, Liu DF, Guan Y, Yi HY, *et al*. Tonoplast-localized nitrate uptake transporters involved in vacuolar nitrate efflux and reallocation in Arabidopsis. Scientific Reports. 2017; 7: 6417. https://doi.org/10.1038/s41598-017-06744-5.
[56] Huang W, Bai G, Wang J, Zhu W, Zeng Q, Lu K, *et al*. Two Splicing Variants of *OsNPF7.7* Regulate Shoot Branching and Nitrogen Utilization Efficiency in Rice. Frontiers in Plant Science. 2018; 9: 300. https://doi.org/10.3389/fpls.2018.00300.
[57] Chen CZ, Lv XF, Li JY, Yi HY, Gong JM. Arabidopsis NRT1.5 is another essential component in the regulation of nitrate reallocation and stress tolerance. Plant Physiology. 2012; 159: 1582–1590. https://doi.org/10.1104/pp.112.199257.